# Carbon Foam Decorated with Silver Nanoparticles for Electrochemical CO_2 Conversion

Sichao Ma,[a, b] Jianfeng Liu,[b] Kazunari Sasaki,[b] Stephen M. Lyth,*[b] and Paul J. A. Kenis*[a, b]

Electrochemistry is a promising method to recycle CO_2 into useful carbon feedstock and for storing intermittent renewable energy. To date, Au and Ag nanoparticles are the most active catalysts for electrochemical conversion of CO_2 to CO. However, agglomeration reduces the activity and the high cost slows widespread commercialization. Suitable support materials are thus needed to improve catalyst utilization. We explore carbon foam (CF) as a catalyst support. Compared with carbon black or graphene nanoplatelets, CF has higher surface area, larger pores, and more defects, resulting in improved uniformity of Ag nanoparticle distribution as well as higher activity and efficiency for CO_2 conversion to CO.

Atmospheric CO_2 levels have increased significantly, and this has been linked to climate change, erratic weather patterns, increasing temperatures, and rising sea levels. Renewable energy sources such as wind and solar are being implemented at large scale to lower carbon emissions.[1] However, the intermittency of such technologies hinders their widespread adoption as they are not always available when demand is high. Electroreduction of CO_2 to CO using off-peak renewable energy has potential to directly reduce CO_2 emissions, create fuels or chemical precursors, and act as an energy storage medium to smooth out supply and demand.[2] Noble metals such as Ag and Au are highly active for the electrochemical conversion of CO_2 to CO.[2a,3] However, suitable catalyst support materials with high electrical conductivity, suitable porosity, and good stability are necessary to improve catalyst utilization and reduce cost.[4] We previously developed carbon foam (CF) as a Pt catalyst support for fuel cells.[5] Large surface area and good nanoparticle (NP) distribution resulted in high electrochemical surface area and oxygen reduction reaction activity. Such CF may thus also be suitable as an Ag support for the electroreduction of CO_2. Here, we report the synthesis of silver-decorated CF for electroreduction of CO_2 to CO.

[a] S. Ma, Prof. P. J. A. Kenis
School of Chemical Sciences
University of Illinois at Urbana-Champaign
600 South Mathews Avenue, Urbana, IL 61801 (USA)
E-mail: kenis@illinois.edu

[b] S. Ma, J. Liu, Prof. K. Sasaki, Prof. S. M. Lyth, Prof. P. J. A. Kenis
International Institute for Carbon-Neutral Energy Research (WPI-I2CNER)
Kyushu University
744 Moto-oka, Nishi-ku, Fukuoka 819-0395 (Japan)
E-mail: lyth@i2cner.kyushu-u.ac.jp

The ORCID identification number(s) for the author(s) of this article can be found under http://dx.doi.org/10.1002/ente.201600576.

This publication is part of a Special Issue on "CO_2 Utilization". To view the complete issue, visit: http://dx.doi.org/10.1002/ente.v5.6

Scanning electron microscope (SEM) images (Figure 1) show that CF has a highly porous carbon network with µm-scale voids and thin, graphene-like cell walls. In contrast, commercial graphene nanoplatelets (CG) comprise µm-scale agglomerates of restacked graphene sheets whilst carbon
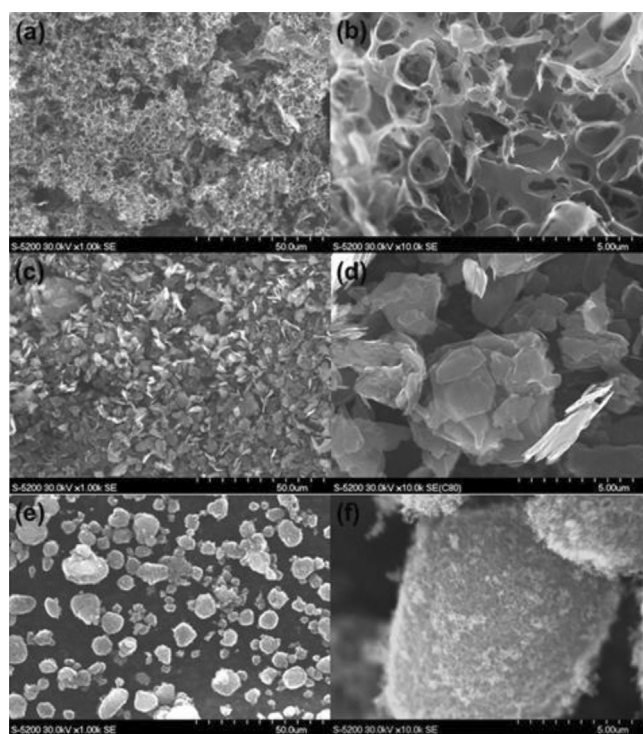
Figure 1. SEM images of (a, b) CF, (c, d) CG, and (e, f) CB. Scale bars correspond to 50 (a, c, e) and 5 µm (b, d, f).

black (CB) forms $\approx$5–20 µm agglomerates with a primary particle size of $\approx$40 nm. Brunauer–Emmett–Teller (BET) nitrogen adsorption reveals surface areas of 904, 652, and 237 $m^2 g^{-1}$ for CF, CG, and CB, respectively. CF has by far the highest surface area. CB and CG have broad pore-size distribution (Figure 2a) whereas CF mainly has pore radii of <2 nm in addition to the micrometer-scale pores observed by SEM.

Raman spectra for CF, CG, and CB are shown in Figure 2b. The G peaks at 1592, 1574, and 1582 cm^{-1}; the G-peak full-width-at-half-maximum (FWHM) of 85.8, 63.4, and 88.9 cm^{-1}; and the I_D/I_G ratios of 0.99, 0.95, and 1.04, respectively, indicate that CF has a high degree of disorder similar to CB whereas CG is a more crystalline material.[6,7]

The morphology and distribution of Ag nanoparticles formed on the support surface was investigated using trans-
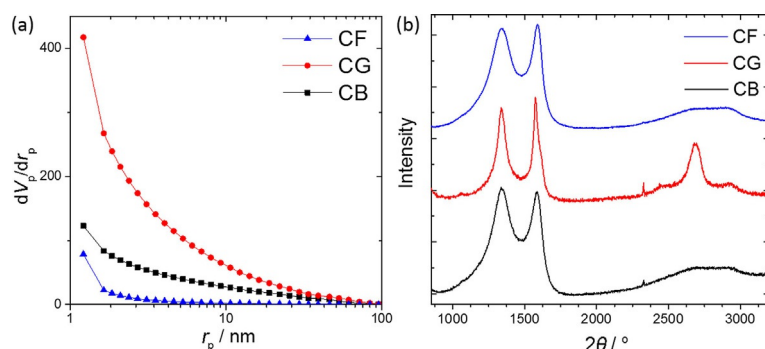
Figure 2. (a) Pore-size distributions and (b) Raman spectra of the CF, CG, and CB samples.

mission electron microscopy (TEM, Figure 3). The sheet-like structure of both CF and CG is clearly observed whereas CB is formed of spheroidal carbon NPs with ≈40 nm diameter. Ag NPs with a diameter of ≈5 nm are formed and distributed uniformly across the surface of Ag/CF (several larger particles are also observed). In contrast, the NPs are much larger (>20 nm) and have poor distribution in both Ag/CG and Ag/CB. The difference in Ag distribution is attributed to the larger surface area of CF and the higher degree of disorder providing numerous anchoring sites for NP nucleation at edges and defects.

The catalytic activity towards electrochemical CO_2 reduction was measured in a flow reactor.[4a,8] Figure 4a shows partial current densities for CO production (j_{co}). Ag/CF has by far the highest (≈120 mA cm^{-2} at −2.06 V$_{Ag/AgCl}$), followed by Ag/CG (≈58 mA cm^{-2}), and Ag/CB (≈30 mA cm^{-2}). The differences are mainly driven by the Faradaic efficiency (FE, Figure 4b). Ag/CF has the highest FE (84 % at −1.82 V$_{Ag/AgCl}$), but this drops at more negative potentials, possibly due to Ag agglomeration during operation for high loadings.[4a] The improved performance of Ag/CF is attributed to the porosity, large surface area, and improved NP distribution, leading to increased mass transport and larger triple-phase boundary.[9] Ag/CG performs better than Ag/CB due to its higher electrical conductivity and surface area. Additionally, some Ag NPs may be trapped in the deep pores of CB.[4a] Cyclic voltammetry was performed from 0 to −1.8 V vs. Ag/AgCl in a standard three-electrode cell with 0.5 M KHCO$_3$ electrolyte (data not shown). This showed that Ag/CF has
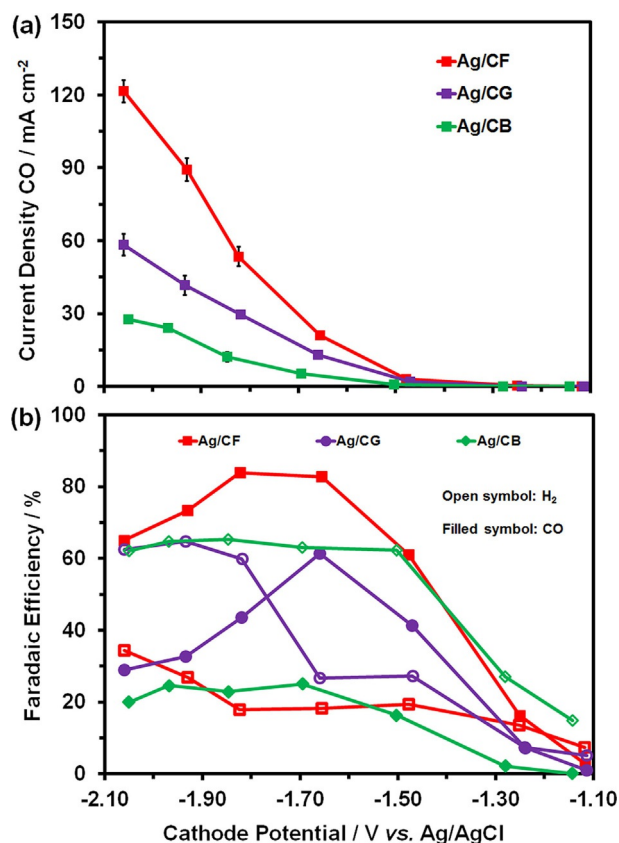

Figure 4. Flow-cell results for Ag/CF, Ag/CG, and Ag/CB: (a) partial current density for CO and (b) Faradaic efficiency.
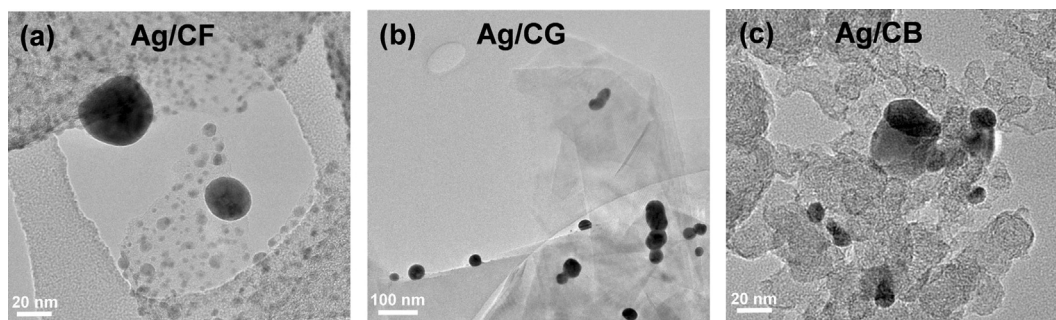

Figure 3. TEM images of (a) Ag/CF, (b) Ag/CG, and (c) Ag/CB.

the highest double-layer capacitance, which may contribute to enhanced desorption of key reaction intermediates, further promoting CO formation and resulting in the improved performance.

In summary, carbon foam (CF) was utilized as a high-performance Ag catalyst support for electrochemical CO_2 conversion to CO, far outperforming CG and CB, with high partial current density and Faradaic efficiency. The improved activity is attributed to the large surface area and porosity as well as to the improved catalyst nanoparticle distribution.

Experimental Section

CF was synthesized by thermal decomposition of sodium ethoxide (Wako) in air.[4a,5,10] The resulting powder was crushed, sonicated, and washed in deionized water to remove NaOH, then pyrolysed at $600\,°C$ for 2 h under N_2 flow. The citrate-protecting method was used for Ag decoration.[4a,10,11] CF or CG (Graphene Supermarket, Grade 4; 80 mg) were mixed with $AgNO_3$ solution (188.6 mg $AgNO_3$ in 18.5 mL H_2O, $AgNO_3$ solid from Sigma–Aldrich), and stirred for 30 min. Sodium citrate solution (Fisher Chemicals, 131 mM, 18.5 mL aqueous solution) was added dropwise, then $NaBH_4$ solution (Sigma–Aldrich, 30 mM, 37.5 mL aqueous solution) was added while stirring vigorously in an ice-bath to reduce Ag^+ to Ag. After gentle stirring overnight, the product was centrifuged, washed, and dried under vacuum at $80\,°C$ for 4 h. Ag/CB was used as? (60 wt %, E-Tek). Characterization was done by SEM (S-5200, Hitachi), TEM (JEOL 2100 CRYO, 200 kV), BET nitrogen adsorption (Belsorp mini II-VS, Bel Japan, Inc.), and Raman spectroscopy (DM2500M, Renishaw, UK, $\lambda = 532$ nm). Ag loading was determined by inductively coupled plasma atomic emission spectroscopy (ICP-AES) (PerkinElmer-Optima 2000DV) to be 57.4 % for CF and 53.3 % for CG.

Cathode catalyst inks were prepared by sonicating Millipore water (200 μL), electrocatalyst powder (2 mg), Nafion® solution (2.6 μL, 5 wt %, Fuel Cell Earth), and isopropyl alcohol (200 μL) for 15 min. The ink was painted onto Sigracet 35 BC gas diffusion layers (GDLs, Ion Power, 1 cm^2) with a loading of 1 mg cm^{-2}. The anode loading was also 1 mg cm^{-2} (IrO_2).[12] The flow reactor was operated under ambient conditions.[4a,8] A potentiostat (Autolab PGSTAT-30, EcoChemie) operating in steady-state chronoamperometric mode was used to measure the current.[4a,13] Seven cell potentials were applied, and the product gas was sampled after a steady state was reached (200 s). The current was then averaged over 180 s before changing the potential. Electrode potentials were measured with multimeters (AMPROBE 15XP-B) connected to each electrode and an Ag/AgCl reference electrode (RE-5B, BASi) downstream. CO_2 was introduced at 7 sccm, and 1 M KOH electrolyte was supplied at 0.5 mL min^{-1}. Gaseous products were extracted through the GDL by vacuum and quantitatively analyzed by gas chromatography (GC, Thermo Finnegan Trace, thermal conductivity detection mode,

He carrier gas). The only cathode products detected were CO and H_2.[14] Partial current densities were calculated by multiplying the total current density by the Faradaic efficiency.

[1] S. Pacala, R. Socolow, *Science* **2004**, *305*, 968–972.
[2] a) Y. Hori in *Modern Aspects of Electrochemistry, Vol. 42* (Eds.: C. Vayenas, R. White, M. Gamboa-Aldeco), Springer, New York, **2008**, pp. 89–189; b) D. T. Whipple, P. J. A. Kenis, *J. Phys. Chem. Lett.* **2010**, *1*, 3451–3458; c) H.-R. M. Jhong, S. Ma, P. J. A. Kenis, *Curr. Opin. Chem. Eng.* **2013**, *2*, 191–199.
[3] Y. Hori, H. Wakebe, T. Tsukamoto, O. Koga, *Electrochim. Acta* **1994**, *39*, 1833–1839.
[4] a) S. Ma, Y. Lan, G. M. J. Perez, S. Moniri, P. J. A. Kenis, *ChemSusChem* **2014**, *7*, 866–874; b) T. Yamamoto, D. A. Tryk, K. Hashimoto, A. Fujishima, M. Okawa, *J. Electrochem. Soc.* **2000**, *147*, 3393–3400; c) N. P. Lebedeva, V. Rosca, G. J. M. Janssen, *Electrochim. Acta* **2010**, *55*, 7659–7668.
[5] J. Liu, D. Takeshi, K. Sasaki, S. M. Lyth, *J. Electrochem. Soc.* **2014**, *161*, F838–F844.
[6] a) N. Ferralis, *J. Mater. Sci.* **2010**, *45*, 5135–5149; b) J.-K. Shin, C. S. Lee, K.-R. Lee, K. Y. Eun, *Appl. Phys. Lett.* **2001**, *78*, 631–633.
[7] R. C. Chatelier, H. A. W. St John, T. R. Gengenbach, P. Kingshott, H. J. Griesser, *Surf. Interface Anal.* **1997**, *25*, 741–746.
[8] D. T. Whipple, E. C. Finke, P. J. A. Kenis, *Electrochem. Solid-State Lett.* **2010**, *13*, B109–B111.
[9] R. O'Hayre, D. M. Barnett, F. B. Prinz, *J. Electrochem. Soc.* **2005**, *152*, A439–A444.
[10] J. Guo, A. Hsu, D. Chu, R. Chen, *J. Phys. Chem. C* **2010**, *114*, 4324–4330.
[11] S. Maheswari, P. Sridhar, S. Pitchumani, *Electrocatalysis* **2012**, *3*, 13–21.
[12] S. Ma, R. Luo, S. Moniri, Y. Lan, P. J. A. Kenis, *J. Electrochem. Soc.* **2014**, *161*, F1124–F1131.
[13] C. E. Tornow, M. R. Thorson, S. Ma, A. A. Gewirth, P. J. A. Kenis, *J. Am. Chem. Soc.* **2012**, *134*, 19520–19523.
[14] a) E. J. Dufek, T. E. Lister, S. G. Stone, M. E. McIlwain, *J. Electrochem. Soc.* **2012**, *159*, F514–F517; b) E. J. Dufek, T. E. Lister, M. E. McIlwain, *Electrochem. Solid-State Lett.* **2012**, *15*, B48–B50.